RSC Advances

ROYAL SOCIETY OF CHEMISTRY

www.rsc.org/advances

Graphical Abstract:

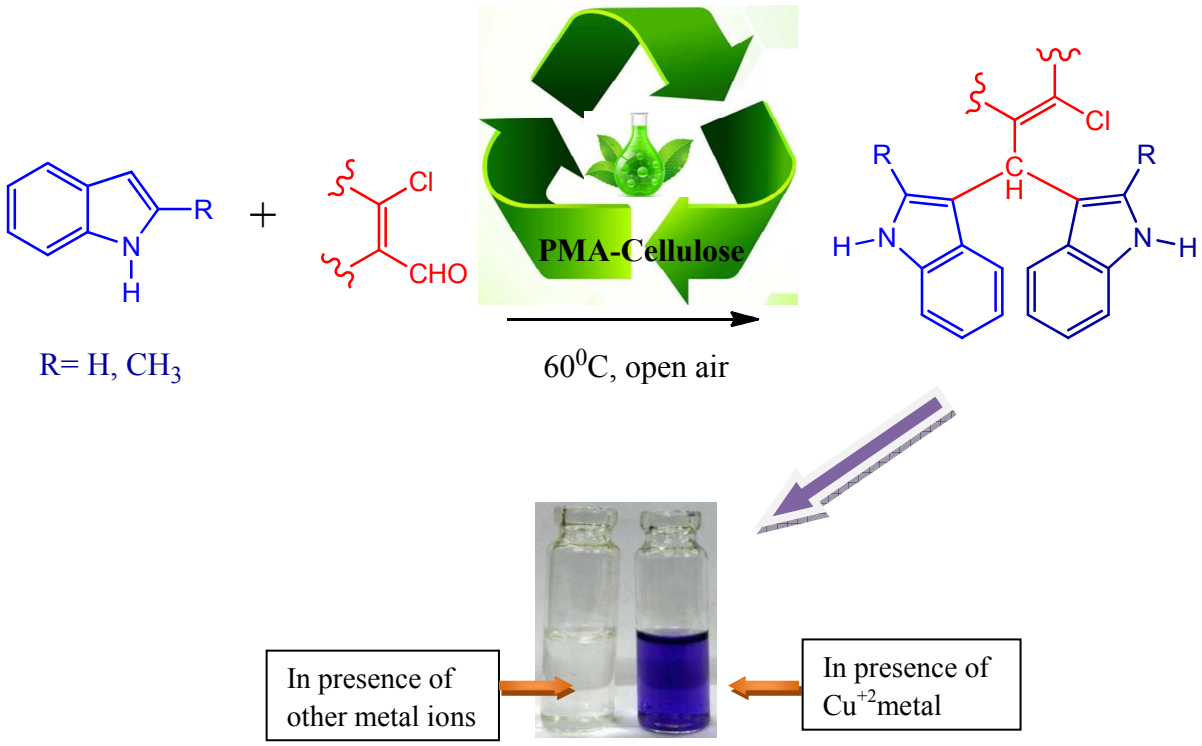

A green one pot synthesis of novel bis(indolyl)methanes as naked eye chemosensors towards Cu^{2+} ion had been developed from β-chloro-α,β-unsaturated aldehydes using new reusable solid acid support/catalyst PMA-Cellulose.

An efficient solvent-free synthesis of bis(indolyl)methane-based naked eye chemosensor for Cu^{2+} ion from β-chloro-α,β-unsaturated aldehydes using PMA-Cellulose as solid phase reusable catalyst

Arijit Kundu[a], Aniruddha Ganguly[b], Kaliprasanna Dhara[b*], Prasanta Patra[c] and Nikhil Guchhait[b]

[a] *Department of Chemistry, Maulana Azad College, Kolkata-700013, India*

[b] *Department of Chemistry, University College of Science and Technology, University of Calcutta, Kolkata-700009, India,*

[c] *Department of Chemistry, Jhargram Raj College, Paschim Medinipur-721507, India*

Abstract:

Realistically designed bis(indolyl)methanes from β-chloro-α,β-unsaturated aldehydes exhibited remarkable naked eye sensitivity towards Cu^{2+} ion. A green one pot technique has been developed for their synthesis using PMA-Cellulose as reusable solid acid support/catalyst under solvent free condition. The procedure offered excellent yields within a short period of time.

Key Words:

β-chloro-α,β-unsaturated aldehydes, indole, bis(indolyl)methane, PMA-Cellulose, Cu^{2+} sensor

Corresponding author. Tel +919433166973

E-Mail: chemkpd@gmail.com

Introduction:

Modulation of the design of new host molecule as cation sensor – usually a metal ion – has attracted considerable research attention in recent years.[1] Especially, the detection of divalent copper ions at very low level of concentration has gained much importance. The interest was driven by the fact that, among the essential heavy metal ions, Cu^{2+} plays a crucial role in a variety of fundamental physiological processes of living organisms ranging from bacteria to mammals.[2] At the same time, Cu^{2+} is toxic towards biological systems and associated with serious neurological disorders *viz*. Menkes and Wilson diseases,[3] amyotrophic lateral sclerosis,[4] Alzheimer's disease[5] and prion diseases.[6] For these reasons, a number of chromogenic and fluorescent chemo-sensors had been designed for the detection of divalent copper ion. Some bis(indolyl)methane (BIM) derivatives have shown sensitivity towards both anions and cations depending on the nature of the substituents on their molecular architecture.[7,8] Acidic nature of the pyrrolic-NH group in indole-based receptors showed higher binding affinity for anions[7] while incorporation of electron donating group in indolyl system lowered anion affinity and augmented the affinity towards cation.[8] The cation-binding ability of the aforesaid structure might depend upon the electron donating power of the coordinating nitrogen atom and/or availability of π-electron density for complexation.[9] Molina e*t al.*[10] and Kaur and Singh *et al.*[11] had reported certain type of BIM skeleton as efficient chromogenic and fluorescent moiety for Cu^{2+} ion sensing. In this context, the exploration of a new scaffold of Cu^{2+} recognition by modulating the electron donating ability of π-electron cloud

attached to BIM skeleton would be rewarding. It was envisaged that the incorporation of vinylic chlorine group in the novel class of BIM derivatives using β-chloro-α,β-unsaturated aldehydes as the source of carbonyl group could achieve the purpose. In addition, introduction of different electron donating and withdrawing groups on aromatic ring attached to π-electron system would sensitively alter their response towards Cu^{2+} sensing.

As catalysis is the soul of innumerable chemical processes, in the aspect of green chemistry, search for green protocol with pollution free catalysts is another exciting area of research. Now-a-days, solid acidic support/catalyst has received significant attention in organic synthesis due to several advantages like easy separation procedure, environmental compatibility, low cost, non-toxicity and high selectivity etc. A number of solid support/catalyst such as HBF_4-SiO_2, ZnO, SiO_2-$AlCl_3$, Silica gel, Silica-Sulphuric Acid, M K10 Clay, Fe/Al-pillard Clay etc. were used for the synthesis of BIM derivatives.[12] Heteropolyacids (HPAs) had emerged as relevant solid acid catalysts for their green benefits and potential economic value.[13] HPAs with their Keggin structure were extensively studied among polyoxometalate class and were shown to possess relatively high thermal stability and high intrinsic Brönsted acidity comparable to super acids.[14] Due to low specific surface area of HPAs (1-10 m^2/g) it is necessary to increase the number of accessible acid sites for better catalytic activity. This can be accomplished by dispersing HPAs on solid support having high surface area. We have chosen cellulose as solid support, a green inexpensive biodegradable natural polymer having long chain β-1,4-glucan.[15] It is also expected that the hydroxyl groups on cellulose surface might enhance the acidity of HPAs through certain intermolecular processes. Synthesis of targeted BIM derivatives under solvent free condition was carried out by optimizing phosphomolybdic acid (PMA) as suitable HPA on cellulose support (PMA-Cellulose) as a solid acid support/catalyst.

Some instances of solid supported PMA catalyzed organic transformations was reported where in every cases organic solvent was used as an obvious ingredient for the reaction.[16] We have used PMA-Cellulose in absence of any solvent for the synthesis of BIM derivatives. To the best of our knowledge this is the first account of the use of PMA-Cellulose as a solid acid support/catalyst and also β-chloro-α,β-unsaturated aldehydes derivatives as sources of carbonyl groups for the syntheses of BIM derivatives (**Scheme 1 and 2**).

Result and discussion

The synthesis of PMA-Cellulose has been discussed in the experimental section. Several distinctive features of PMA-Cellulose were observed. Initially the formation of PMA-Cellulose was established by IR spectroscopy (see supplementary **Fig-S1**). The exact crystal plane of PMA-Cellulose and reused PMA-Cellulose were estimated by X-ray diffraction (XRD) analysis (see supplementary **Fig-S2**) applying Sherrer's formula $D_p = 0.941\lambda/\beta \cos\theta$; where X-ray wave length (λ) = 1.5406 Å, θ = Bragg′s diffraction angle for the plane (110), (210), (221), (311), (321), (420), (332), (422), (620) etc and β is the corresponding full width at half maximum (FWHM) value. Field Emission Scanning Electron Microscopy (FESEM) was used for determining the surface morphology of PMA-Cellulose before and after use in reaction **(Fig- 1a, 1c)**. EDX study of PMA-Cellulose was also performed from FESEM **(Fig- 1b)** to determine the elemental composition, which confirmed the presence of Mo. ICP Mass study also supported this result. It is a non-hygroscopic solid with high thermal stability as substantiated from thermo-gravimetric analysis **(Fig-1d)**. To ascertain the binding efficiency of PMA with cellulose, leaching test was performed in ethyl acetate solution where no leaching of PMA was observed.

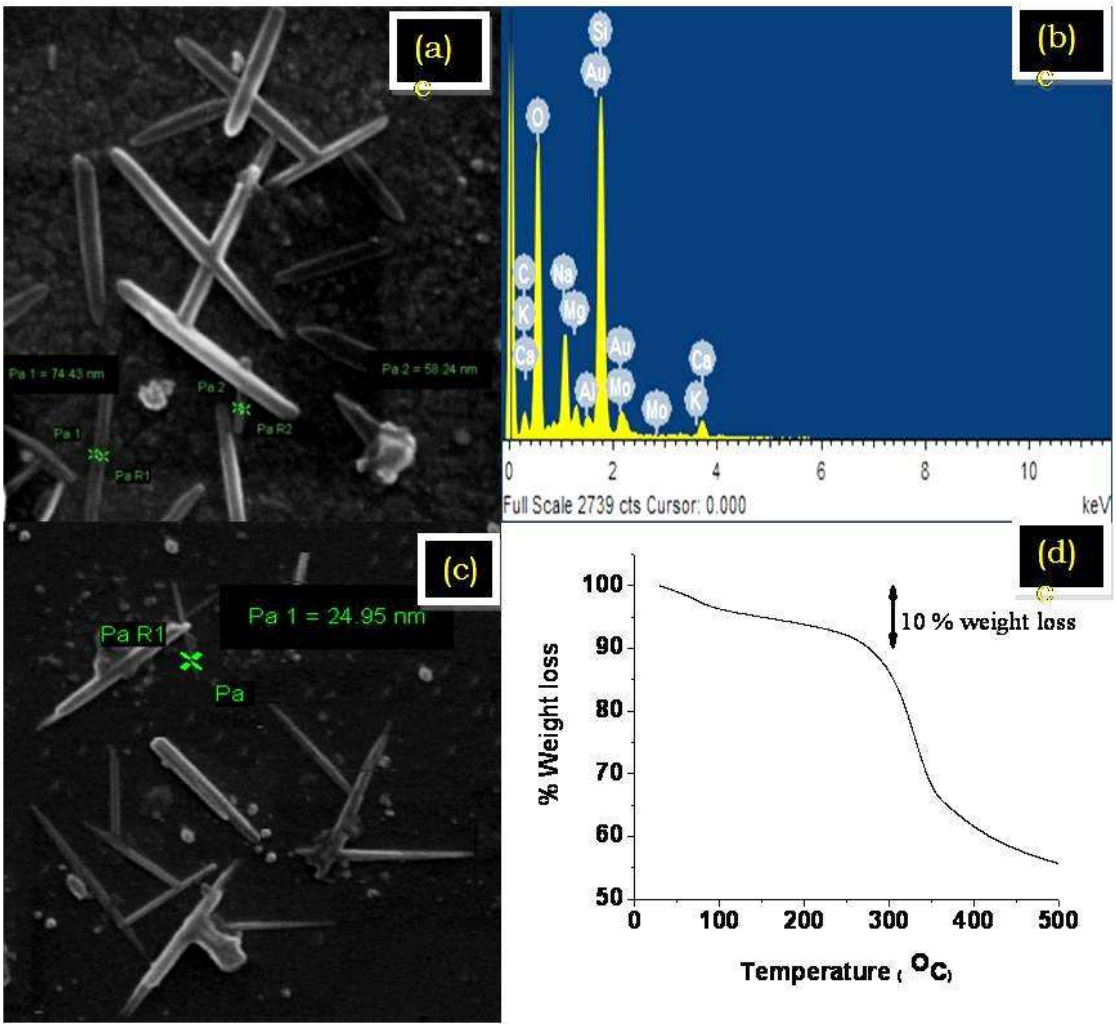

Fig 1: (a) FESEM image of PMA-Cellulose before use; (b) EDX study of PMA-Cellulose using FESEM ; (c) FESEM image of PMA-Cellulose after five time reuse; (d) TGA image of PMA-Cellulose

In order to optimize the suitable reaction condition, we carried out extensive screening tests employing a representative reaction of indole **(1a)** (2.0 mmol) with 3-chloro-3-phenylacrylaldehyde **(2a)** (1.2 mmol) on different solid phase acid catalysts. The reaction parameters such as temperature, amount of catalyst, reaction time etc were also investigated and the outcomes have been summarized in **Table 1**. Initially the reaction was carried out by using phosphomolybdic Acid on SiO_2 surface (PMA-SiO_2, 20 weight %) and phosphotungstic Acid (PTA) on SiO_2 surface (PTA-SiO_2, 20 weight %), but resulted in only a moderate yield of the product even after long

reaction time at 100 ºC (Table 1, entry 1, 2). Literature survey revealed that HPAs on SiO_2 surface at low loading level undergoes decomposition due to interactions with surface silanol groups.[17] Consequently we were in the hunt for a more efficient surface catalytic system with HPAs. Hence we dispersed PTA and PMA on cellulose support. But PTA-Cellulose (10 weight % and 20 weight %) failed to give adequate response after long time at 90°C (Table 1, entry 3, 4), whereas PMA-Cellulose (5 weight %) provided a satisfactory yield of the expected compound within 45 minutes (Table 1, entry 5). Misono *et al.* have studied extensively on the mechanism for reduction of both PTA and PMA with H_2 and explained on the basis of two general equation ($H_2 + PM_{12}O_{40}^{3-} \leftrightarrow 2H^+ + PM_{12}O_{40}^{5-}$…..[I], $2H^+ + PM_{12}O_{40}^{5-} \leftrightarrow H_2O + PM_{12}O_{39}^{3-}$…..[II], M= W or Mo) where H_2 transferred to H_2O. The experiments revealed that the equilibrium strongly favoured the left hand side of equation- I for PTA whereas PMA favoured the right hand side of the equation- I.[18] These observations established the fact of higher reactivity of PMA as oxidant over PTA which also supports the result of better activity of PMA-Cellulose than PTA-Cellulose in this case. We then applied PMA-Cellulose (10 weight %) at same temperature, which marginally enhanced the yield of the desired product (Table 1, entry 6). Henceforth some screening tests were attempted with PMA-Cellulose (10 weight %) for optimizing the best condition by changing the amount of the catalyst (Table 1, entry 7,8,9,12) and the reaction temperature (Table 1, entry 10,11,13). Eventually desired yield was achieved by using 20 mg of PMA-Cellulose (10 weight %) at 60ºC which afforded 96% yield of the desired product (Table 1, entry 11). Using 20 mg of PMA-Cellulose (20 weight %) at 60ºC gave identical yield of the desired product as before (Table 1, entry 15). The effect of the reaction time with the yield of the product was also studied. It indicated that the yield of the product increased with time for a period of 20 min. and then it remained unaltered (see supplementary **Fig-S3**).

To show the extent and limitations of this protocol we investigated the new methodology using different indole systems with various acyclic β-chloro-α,β-unsaturated aldehydes (Table 2) and cyclic β-chloro-α,β-unsaturated aldehydes (Scheme 2, Table 3). In all the cases reaction progressed smoothly with good to excellent yield. The reactions were consistently carried out at the 1 mmol scale and no change of product yield was observed when scaled up to the 10 mmol scale.

Table 1: Optimization study using **1a** and aldehyde **2a**

Entry	Solid Phase Catalyst	Temperature(°C)	Amount (mg)	Time	Yield[a,b] (%)
1.	PMA-SiO_2 (20%)	100	70	8.5hrs	35
2.	PTA-SiO_2 (20%)	100	70	9hrs	30
3.	PTA-Cellulose (10%)	100	70	5hr	40
4.	PTA-Cellulose (20%)	100	70	5hr	45
5.	PMA-Cellulose (5%)	90	50	45min	70
6.	PMA-Cellulose (10%)	90	50	35min	80
7.	PMA-Cellulose (10%)	90	70	45min	80
8.	PMA-Cellulose (10%)	90	30	35 min	87
9	PMA-Cellulose (10%)	90	20	35 min	90
10.	PMA-Cellulose (10%)	80	20	20 min	96
11.	**PMA-Cellulose (10%)**	**60**	**20**	**20 min**	**96**
12.	PMA-Cellulose (10%)	60	10	20 min	85
13.	PMA-Cellulose (10%)	50	20	25min	80
14.	PMA-Cellulose (20%)	60	20	20 min	96

[a] all the reactions were carried out with Indole (2.0 mmol) and 3-chloro-3-phenylacrylaldehyde (1.2 mmol). [b] Yield of isolated product.

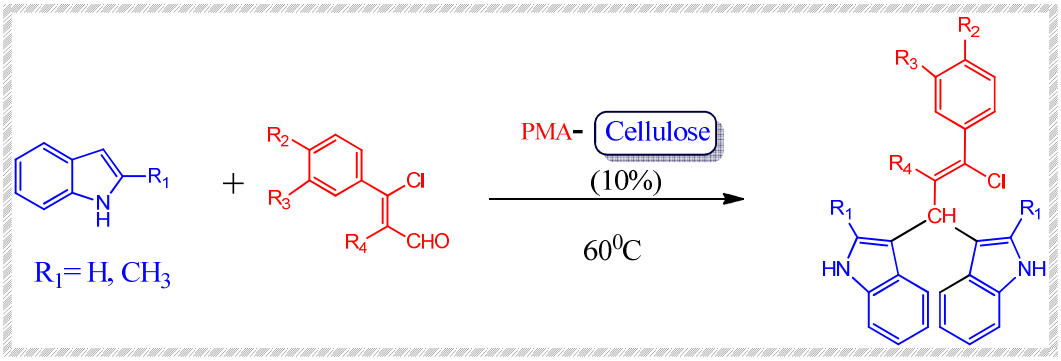

Scheme1: Preparation of BIM derivatives using β-chloro-α,β-unsaturated aldehydes

Table 2: PMA-Cellulose catalysed BIM derivatives of acyclic β-chloro-α,β-unsaturated aldehydes

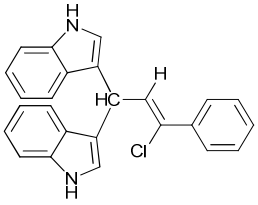

3a, 96%, 20 min

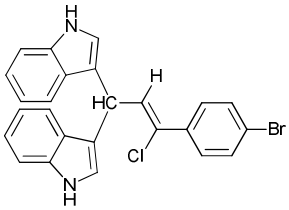

3b, 95%, 23 min

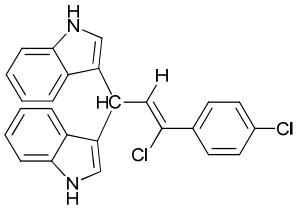

3c, 90%, 21 min

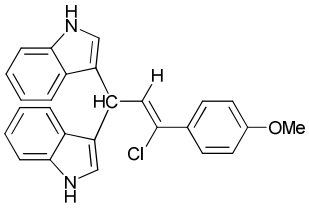

3d, 92%, 23 min

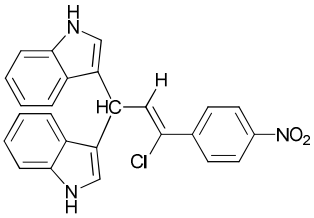

3e, 95%, 20 min

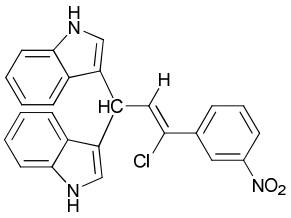

3f, 96%, 25 min

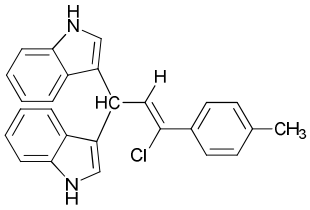

3g, 90%, 24 min

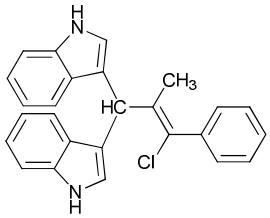

3h, 94%, 20 min

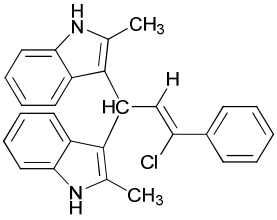

4a, 97%, 24 min

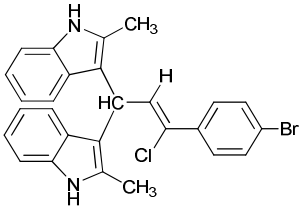

4b, 95%, 20 min

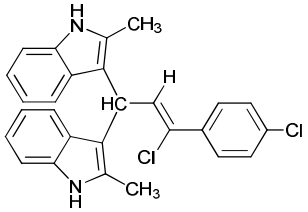

4c, 96%, 25 min

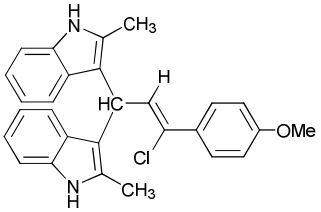

4d, 97%, 23 min

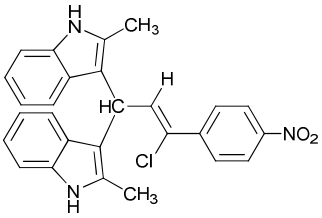

4e, 96%, 20 min

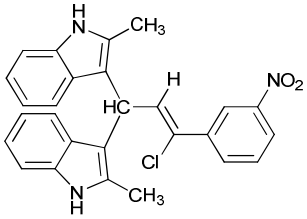

4f, 93%, 20 min

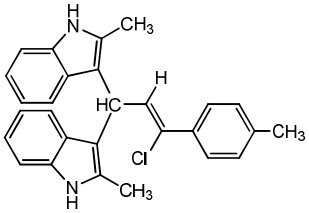

4g, 92%, 25 min

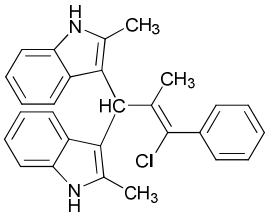

4h, 95%, 20 min

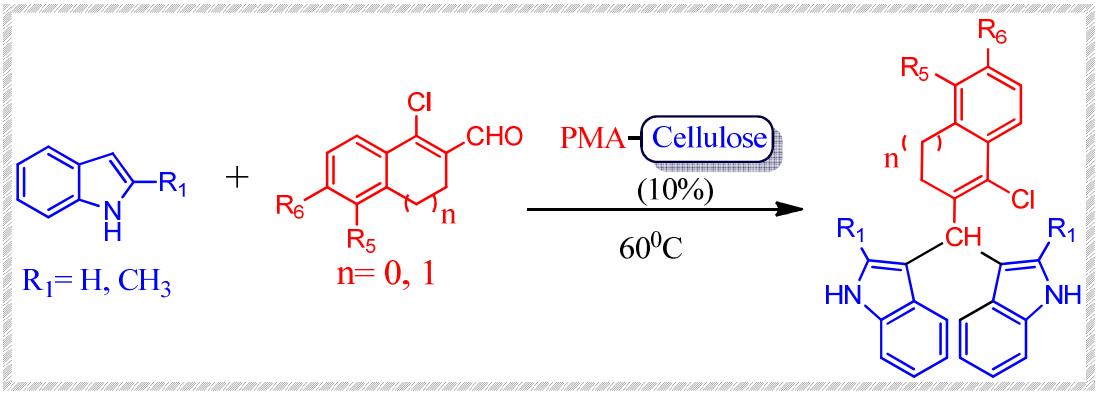

Scheme 2: Preparation of BIM derivative using cyclic β-chloro-α,β-unsaturated aldehydes

Table 3: PMA-Cellulose catalysed BIM derivatives of cyclic β-chloro-α,β-unsaturated aldehydes

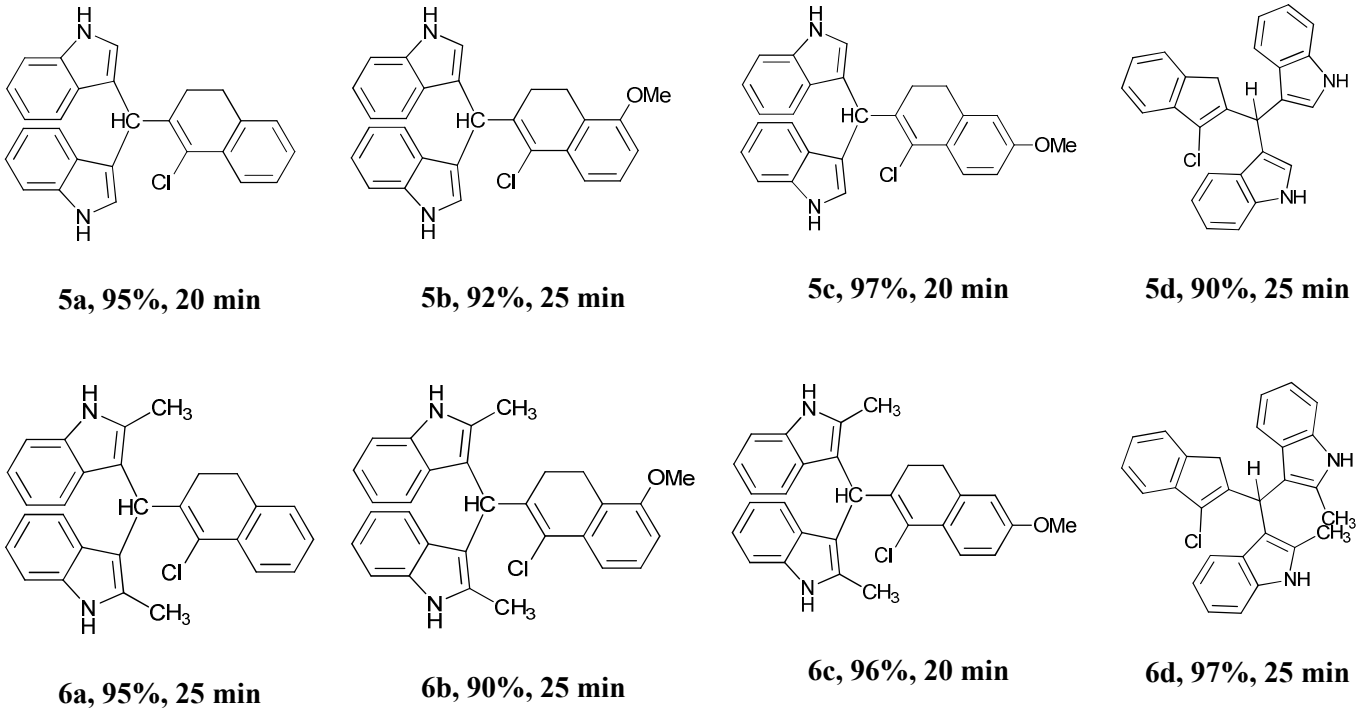

5a, 95%, 20 min | **5b, 92%, 25 min** | **5c, 97%, 20 min** | **5d, 90%, 25 min**

6a, 95%, 25 min | **6b, 90%, 25 min** | **6c, 96%, 20 min** | **6d, 97%, 25 min**

From the perspective of green chemistry, it was fascinating to find that the final products could be isolated from the reaction mixture by dissolving in ethyl acetate and the catalyst was separated simply by filtration due to its insolubility in organic solvent.

A study regarding recovering and reprocessing of PMA-Cellulose was also performed. The isolated solid PMA-Cellulose from ethyl acetate was dried under vacuum and the recovered material was directly used for new reaction. The catalyst was successfully reused six times without any pre-treatment with admirable results (**Fig- 2**). Therefore, we preferred PMA-Cellulose as the solid phase reaction medium over environmentally unsafe organic solvents. Besides, the methodology involved minimization of chemical impurity, easy work-up procedure and nonexistence of large volumes of waste from the discarded chromatographic static phases. The structure of the final products were well characterized by using spectral (IR, ^{1}H and ^{13}C NMR) and elemental analysis data. The structural motif was fully established by single X-ray crystallographic analysis of one signified compound **3b** (CCDC 926789) **(Fig- 3)**.

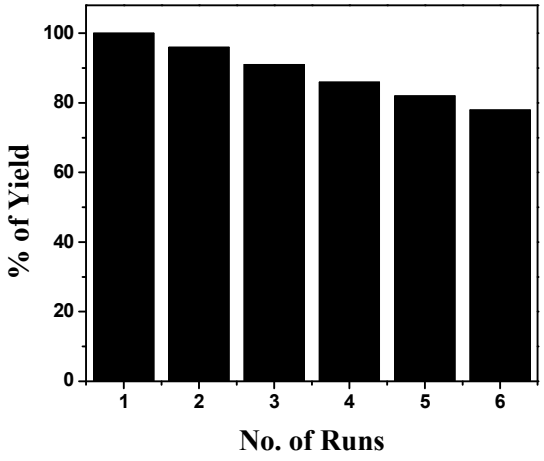

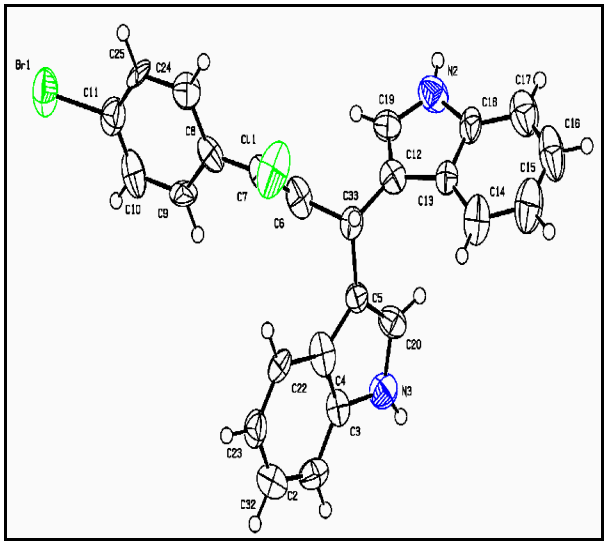

Fig 2: Reusability of PMA-Cellulose **Fig 3**: X-Ray Crystallographic structure of compound **3b**

A plausible mechanistic pathway was proposed to explain the PMA-cellulose catalyzed formation of BIM derivatives (**Fig-4**). It had been indicated form the tertiary structures of HPAs that their acid catalytic property are due to hydrated protons $H^{+}(H_2O)_x$ present in the Keggin structure.[19] Spectroscopic data from ^{1}H- and ^{13}C-NMR of the 'pseudo-liquid phase' of HPAs (arising due to

absorption/adsorption of alcohol) suggested that the hydroxyl groups of alcohol remained protonated with a rapid exchange occurring between the hydroxyl protons of the alcohol and the protons of HPAs.[20] Taking into account these phenomena, it was surmised that the hydroxyl groups on cellulose surface might engage in similar type of protonation *vis-à-vis* proton exchange processes with PMA involving intermolecular interactions through electrostatic forces viz. hydrogen bonding and the surface catalytic activity of PMA-Cellulose was enhanced.

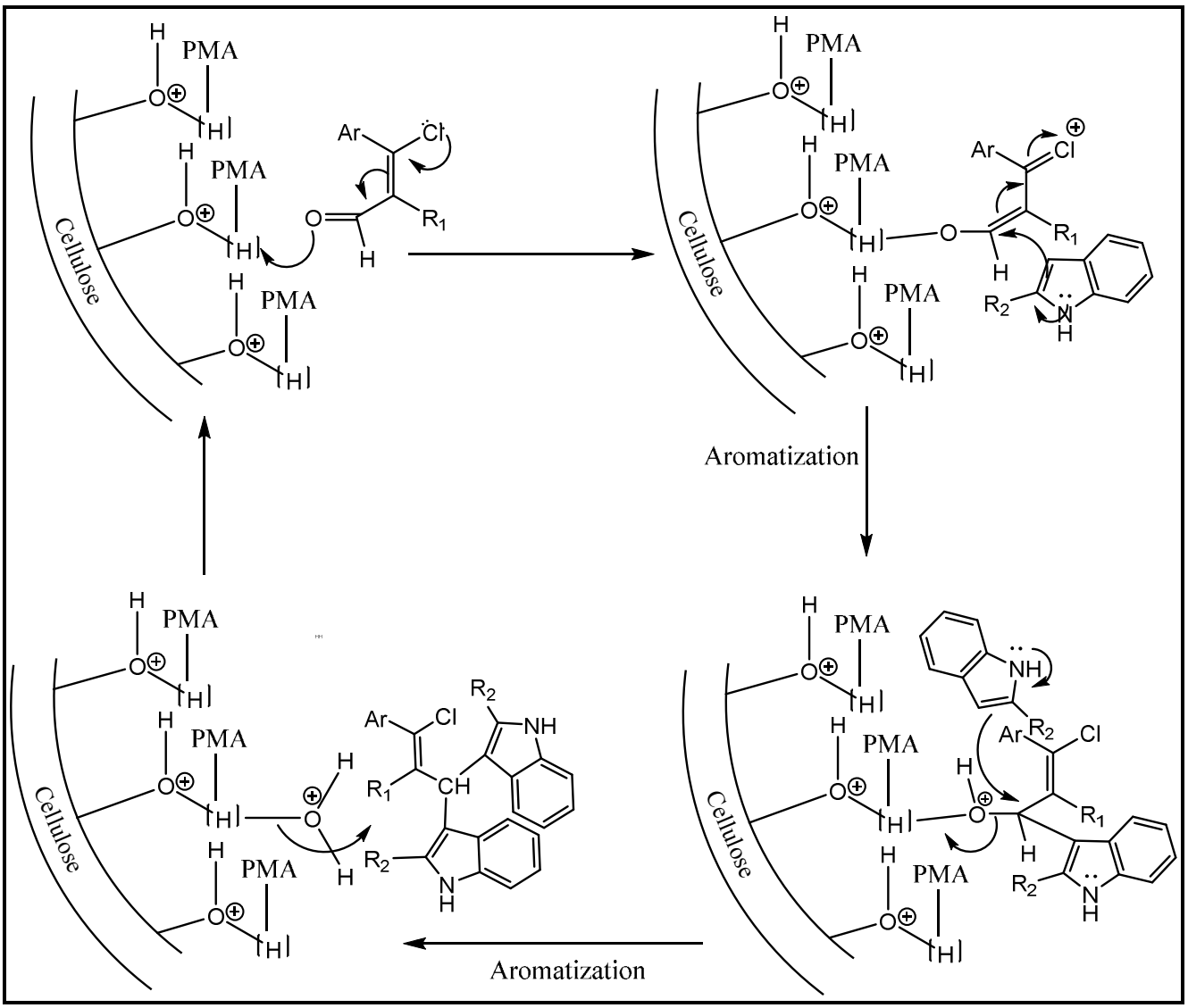

Fig 4: Plausible mechanism for the synthesis of BIM derivatives using PMA-Cellulose as solid phase catalyst

The carbonyl functionalities of β-chloro-α,β-unsaturated aldehydes were activated by those surface available protons of PMA-Cellulose and the reactions proceeds to completion within a short period of time. In addition, presence of vinylic chlorine augmented the electrophilic nature of aldehyde function.

Absorption study:

It is pertinent to mention here that the entire isolated products showed chemosensing properties for Cu^{2+} ion. Of these, 2-methyl indole derivatives exhibited prominent sensitivity compared to unsubstituted indole derivatives, perhaps due to the presence of +I methyl group. We had focused on two compounds **4d** and **4e** which had relatively high quantum yields towards chemosensitivity. The cation sensing property of both **4d** and **4e** were investigated initially by UV-VIS absorption measurements in acetonitrile solvent. The bare compounds **4d** and **4e** revealed characteristic strong absorption bands at ~270 nm which was attributed to the absorption of the indole chromophore present in the molecules under investigation (**Fig- 5)**. In the course of monitoring the effect of transition metal ions on the spectral properties of both the compounds, the absorption spectra were found to remain almost silent to the presence of the transition metal ions (viz. Cd^{+2}, Co^{+2}, Mn^{+2} and Ni^{+2}). As seen in **Fig 5a** and **5b**, gradual addition of Cu^{2+} ion to the solution of both the ligands were found to accompany a decrease in absorbance at ~ 270 nm with a simultaneous emergence of a new band at ~ 580 nm which was supposed to be the signature of a ligand to metal charge transfer (LMCT) state[21], subsequently inducing a prominent colour change from colourless to blue (see supplementary **Fig-S4a**). This result demonstrated the potential of the compounds to distinguish the presence of Cu^{2+} ions in a solution *via* visual inspection only (see supplementary **Fig-S4a**).

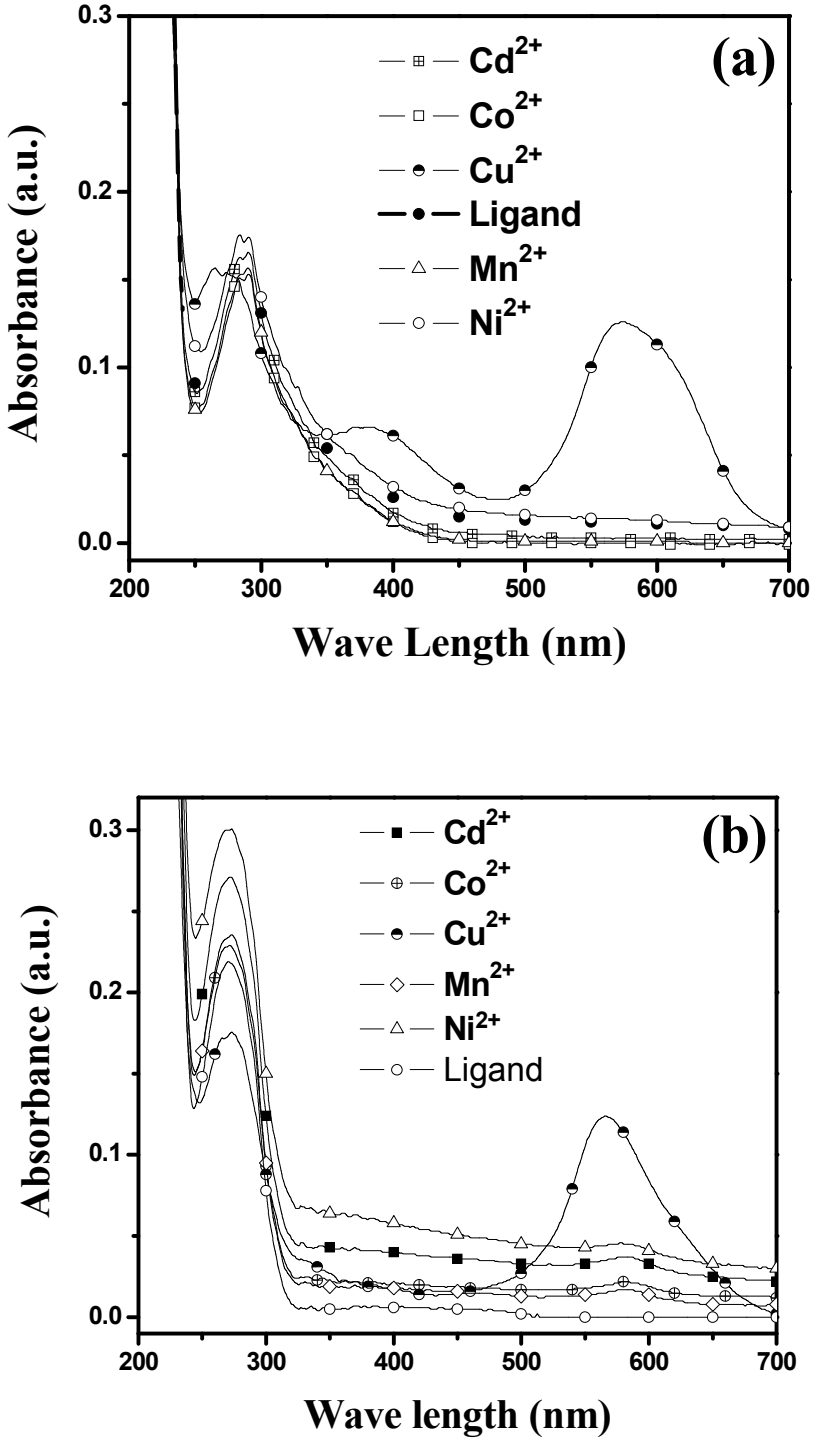

Fig 5: (a) UV-VIS absorption spectra with different metal ion of compound **4d**

(b) UV-VIS absorption spectra with different metal ion of compound **4e**

Studies on interference of other metal ions in presence of Cu^{2+} ion were also carried out using both **4d** and **4e,** which manifested the ability of the aforesaid compounds to sense Cu^{2+} with interference of other bivalent transition metal ions (see supplementary **Fig-S4b**).

Emission study:

Compounds **4d** and **4e**, when excited at their respective absorption maxima in acetonitrile solvent, showed broad unstructured bands with emission maxima at 346 nm and 331 nm. Due to the presence of electron releasing –OMe group, the emission quantum yield of compound **4d** was found to be appreciably higher than its $-NO_2$ substituted analogue **4e**.

Both **4d** and **4e** showed remarkable Cu^{2+} ion selectivity with prominent fluorescence enhancement/quenching. In presence of Cu^{2+} ion, compound **4d** demonstrated a pronounced fluorescence enhancement along with a discernible blue shift (**Fig- 6a**) of the emission band from ~346 nm to ~341 nm, whereas no significant fluorescence change was observed in the presence of other metal ions (**Fig- 6a**). Such an observation of blue shift is often treated as an indication of destabilization of the emissive state.[22,23] It can be concluded that the formed complex was less stable than the free ligand. On the other hand, in case of **4e**, addition of Cu^{2+} ion resulted in a prominent red shift (**Fig- 6b**) of the emission maximum (~331 nm to ~336 nm) with a prominent fluorescence quenching **(Fig- 6b)**. This observation indicated that the complex was more stable than the free ligand.

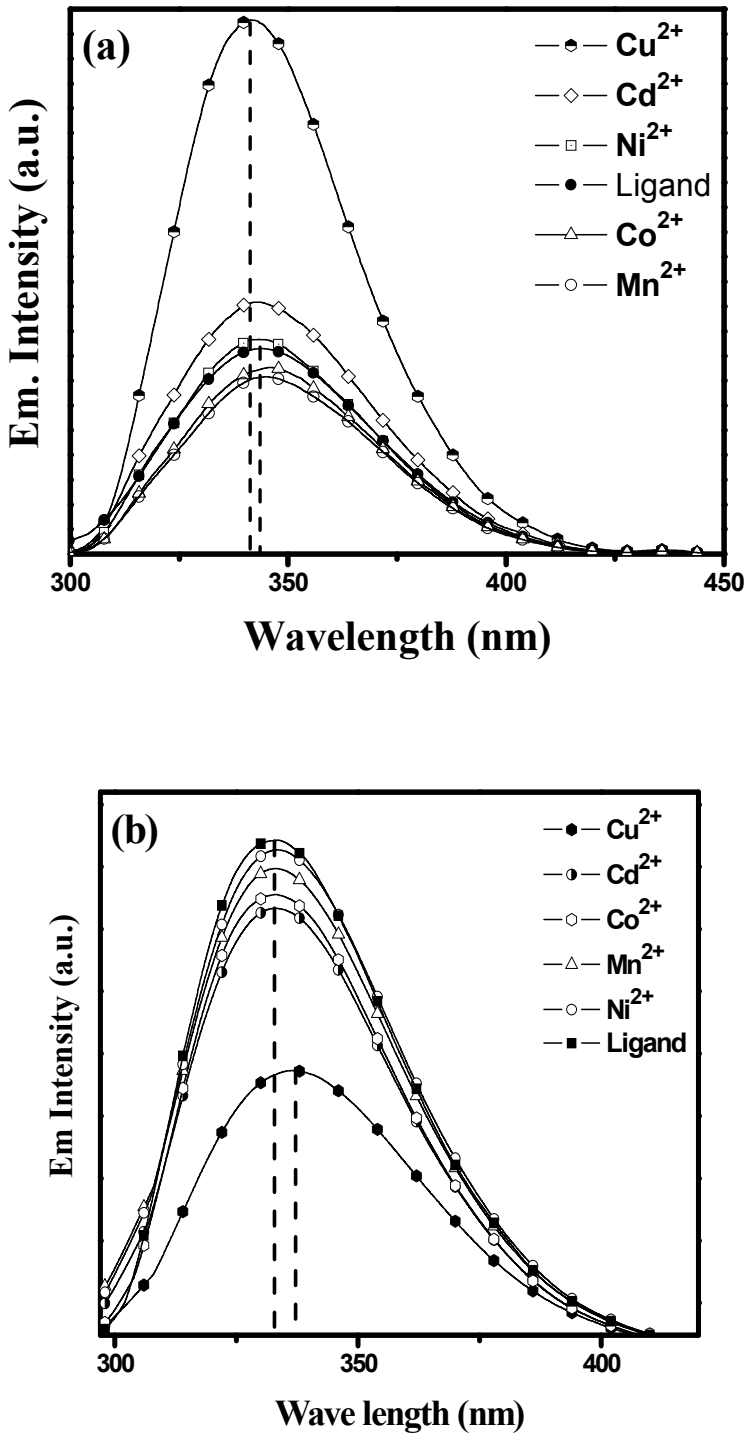

Fig 6: (a) Emission spectra of compound **4d** with different metal ions (λ_{max}= 346 nm)

(b) Emission spectra of compound **4e** with different metal ions (λ_{max}= 331 nm)

It was fascinating to note that both the compounds having functional groups of completely different electronic characters showed exactly opposite behavior on fluorescence study. It may be argued that in case of electron withdrawing $–NO_2$ group, the lack of electron density on the entire emissive framework was replenished possibly due to the presence of Cu^{2+} ion via complexation thereby leading to stabilization. Whereas the electron donating nature of the –OMe group would enrich the electron content of the emissive framework and destabilize the charge transfer complex. However, meticulous inspection of the whole phenomenon is required to further extrapolate the results to arrive at such a conclusion.

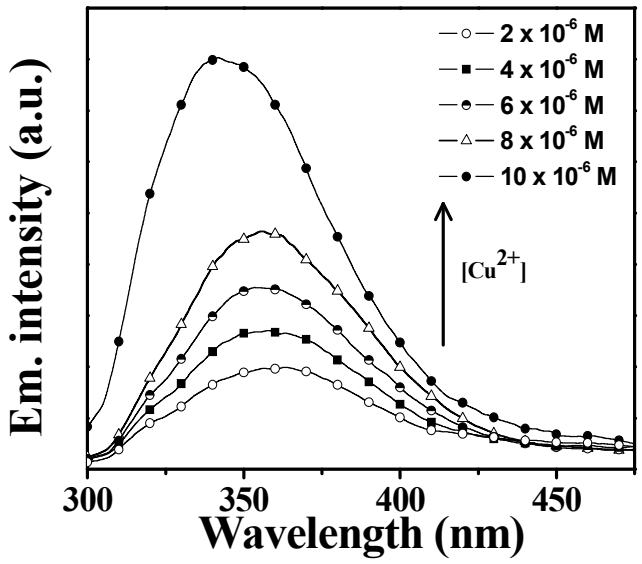

Fig 7: Fluorescence titration spectra for **4e** (c= 1×10^{-5} M) in CH_3CN with copper perchlorate salt (λ_{max}= 331 nm).

In order to find out the binding constant and limit of detection with Cu^{2+} ion, fluorescence titration was performed with the representative compound **4e (Fig-7)**. In general, there are two different types of quenching processes that can occur: static and dynamic. In static quenching, a non-

fluorescent complex is formed between the fluorophore and quencher. In dynamic/collisional quenching, the quencher must diffuse into the excited fluorophore and non-radiatively deactivates the excited state. Both of these quenching processes can be adequately described by the Stern-Volmer equation.[24] For static quenching, which is the case here, the equation can be written as,

$$\frac{I_0}{I} = 1 + K_{SV}[Q]$$

in which I_0 is the original fluorescence intensity; I is the quenched intensity of the fluorophore; Q is the quencher (here Cu^{2+} ion); and K_{SV} is the Stern-Volmer quenching constant. If the Stern-Volmer quenching constants are interpreted as ground-state association constants, then $K_{sv} = K_b$, where K_b is the binding constant of the metal with the fluorophore. The thus determined binding constant for the compound **4e** was calculated to be 1.428 x 10^5 M^{-1} **(**see supplementary **Fig-S5a)** which concludes a strong interaction between the moieties involved. The limit of detection for Cu^{2+} ion was found to be sufficiently low (0.055 ppm) when calculated using the standard procedure **(**see supplementary **Fig-S5b)**.[25]

The efficiency of the new type of BIM derivative towards Cu^{2+} ion sensitivity has been examined by comparing with similar frame where vinylic chlorine was absent. We compared the sensitivity of compound **4a** and bis(indolyl)methane derivative of cinnamaldehyde with 2-methyl indole **(7)**. From the emission study it was observed that in case of compound **7,** there was no change in the intensity of emission band after addition of Cu^{2+} ion at ppm level and only a red shift of the band was observed **(**see supplementary **Fig-S6a)**. No change of colour was observed by naked eye, whereas in case of compound **4a** there was sharp intensification of emission band **(**see supplementary **Fig-S6b)** and acute colour change from colourless to blue was observed after

addition of copper ion. This substantiated the fact that modification in BIM derivatives by introducing vinylic chlorine played a vital role towards Cu^{2+} ion sensing.

Conclusion:

In conclusion, the new class of BIM derivatives showed high chemo-sensing properties towards Cu^{2+} ion at micro molar concentration depending on different electronic characteristics of the substituents and acted as naked eye sensors. A green, chromatography free and product-selective two-component reaction procedure has been developed with PMA-Cellulose as a recyclable solid phase catalyst affording good to excellent yield of the products. Unique choice of aldehydes bearing vinylic chlorine had also been rewarding. One representative molecular structure was investigated by means of X-ray diffraction analysis.

Experimental

Preparation of Catalyst 10%-Phosphomolybdic Acid-Cellulose (PMA- Cellulose)

10 mg of Phosphomolybdic acid was dissolved in 10 ml of methanol. 90 mg of cellulose powder was added to it pinch by pinch for 5 minutes. After completion of addition, the mixture was stirred for four hours and then methanol was evaporated under vacuum. The PMA-Cellulose powder was then air dried and used for the reaction.

Reaction Procedure

2 mmol of indole derivatives and 1.2 mmol of β-chloro-α,β-unsaturated aldehydes were stirred over 20 mg of 10% PMA-Cellulose at 60˚C for 20-30 minutes. The reaction was monitored by TLC. After completion of the reaction the whole mixture was extracted with ethyl acetate and the filtered out PMA-Cellulose was dried under vacuum for reuse. Ethyl acetate part was washed with water thrice and evaporated under vacuum. The solid obtained was washed with ethyl acetate:pet.

ether(5:95, v/v) solution for purification. The products were well characterized by IR, ^{1}H NMR, ^{13}C NMR, elemental analysis and an X-ray crystallographic study.

(Z)-3,3'-(3-(4-bromophenyl)-3-chloroprop-2-ene-1,1-diyl)bis(1H-indole) (3b)

Yield: 95%, (0.439 g); m.p. 163–164°C characteristics: red crystalline solid (from pet. ether-chloroform mix); IR υ_{max} (KBr) 3446, 1481, 1455, 1415, 1337, 1237, 1217, 1095, 1068, 892, 740; ^{1}H NMR (300 MHz, DMSO-D_6) δ_H 5.79 (1H, d, J=9.9 Hz), 6.93-6.98 (2H, m), 7.06-7.11 (2H, m), 7.17 (1H, d, J= 9.9 Hz), 7.31 (1H, s), 7.40 (2H, d, J= 8.1 Hz), 7.56-7.65 (6H, m), 10.97 (2H, s); ^{13}C NMR (75MHz, DMSO-D_6) δ_C 34.7, 112.9, 113.1, 116.2, 117.8, 118.4, 119.9, 120.4, 120.5, 122.1, 122.5, 124.5, 126.7, 127.6, 127.7, 127.9, 129.1, 129.7, 130.8, 131.0, 133.1, 136.9, 137.0; analysis calculated for $C_{25}H_{18}BrClN_2$: C: 65.02; H: 3.93; N: 6.07% found C: 65.01; H: 3.94; N: 6.05%.

Z)-3,3'-(3-chloro-3-(4-methoxyphenyl)prop-2-ene-1,1-diyl)bis(2-methyl-1H-indole) (4d)

Yield: 97%, (0.428g); m.p. 162-163°C characteristics: bluish grey solid; IR υ_{max} (KBr) 3394, 2346, 1601, 1507, 1460, 1289, 1251, 1178, 1023, 834, 739; ^{1}H NMR (300 MHz, DMSO-D_6) δ_H 2.23 (6H, s), 3.66 (3H, S), 5.65 (1H, d, J= 9.6 Hz), 6.69-6.74 (2H, m), 6.83-6.92 (5H, m), 7.14-7.21 (4H, m), 7.49 (2H, d, J= 8.7 Hz), 10.70 (2H, s); ^{13}C NMR (75MHz, DMSO-D_6) δ_C 12.7, 35.4, 55.6, 110.9, 111.4, 118.6, 120.2, 127.6, 127.8, 129.2, 129.6, 130.0, 131.9, 135.5, 159.93; analysis calculated for $C_{28}H_{25}ClN_2O$: C: 76.26; H: 5.71; N: 6.35% found C: 76.24; H: 5.73; N: 6.34%.

(Z)-3,3'-(3-chloro-3-(4-nitrophenyl)prop-2-ene-1,1-diyl)bis(1H-indole) (4e)

Yield: 96%, (0.438g); m.p. 130-131°C characteristics: yellow solid; IR υ_{max} (KBr) 3381, 1593, 1513, 1459, 1343, 849, 747; ^{1}H NMR (300 MHz, $CDCl_3$) δ_H 2.25 (6H, s), 5.84, 6.93 (2H, t, J_1= 7 Hz, J_2= 7.9 Hz), 7.06 (2H, t, J1= 7.8 Hz, J2= 7.3 Hz), 7.18 (1H, d, J= 9.4 Hz), 7.26 (3H, d, J= 7.7

Hz), 7.37 (2H, d, J= 8 Hz), 7.71-7.80 (4H, m), 8.14 (2H, d, J= 8.9 Hz); ^{13}C NMR (75 MHz, $CDCl_3$) δ_C 18.39, 35.7, 58.4, 110.3, 111.4, 118.9, 119.4, 120.9, 123.6, 127.0, 128.2, 134.6, 135.1, 144.0; analysis calculated for $C_{27}H_{22}ClN_3O_2$: C: 71.13; H: 4.86; N: 9.22% found C: 71.14; H: 4.84; N: 9.21%.

Acknowledgements

We gratefully acknowledge the financial support received from the University of Calcutta. Crystallography was performed at the DST-FIST, India-funded Single Crystal Diffractometer facility at the Department of Chemistry, University of Calcutta. We would like to thank the Centre for Research in Nanoscience and Nanotechnology, University of Calcutta for providing FESEM facilities. We express our gratitude to the Geological survey of India, Central Chemical Laboratory, Kolkata for ICP Mass study.

Supplementary Materials

Supplementary data associated with this article can be found in the online version.

Referances:

1. (a) A. P. De Silva, H. Q. N. Gunaratne, T. Gunnlaugsson, A. J. M. Huxley, C. P. McCoy, J. T. Rademacher and T. E. Rice, *Chem. Rev.*, 1997, **97**, 1515; (b) L. Prodi, F. Bolletta, M. Montalti and N. Zaccheroni, *Coord. Chem. Rev.*, 2000, **205**, 59; (c) B. Valeur and I. Leray, *Coord*. *Chem. Rev.*, 2000, **205**, 3; (d) A. P. De Silva, D. B. Fox, A. J. M. Huxley and T. S. Moody, *Coord. Chem. Rev.*, 2000, **205**, 41.
2. (a) M. C. Linder and M. Hazegh-Azam, *Am. J. Clin. Nutr.* 1996, **63**, 797S; (b) R. Uauy, M. Olivares and M. Gonzalez, *Am. J. Clin. Nutr.* 1998, **67**, 952S.

3. (a) C. Vulpe, B. Levinson, S. Whitney, S. Packman and J. Gitschier, *Nat. Genet.* 1993, **3**, 7; (b) P. C. Bull, G. R. Thomas, J. M. Rommens, J. R. Forbes and D. W. Cox, *Nat. Genet.* 1993, **5**, 327.
4. (a) J. S. Valentine and P. J. Hart, *Proc. Natl. Acad. Sci. U.S.A.*, 2003, **100**, 3617; (b) L. I. Bruijn, T. M. Miller, D. W. Cleveland, *Annu. Rev. Neurosci.* 2004, **27**, 723.
5. K. J. Barnharn, C. L. Masters and A. I. Bush, *Nat. Rev. Drug Discov*. 2004, **3**, 205.
6. D. R. Brown and H. Kozlowski, *J. Chem. Soc, Dalton Trans.,* 2004, 1907.
7. (a) F. G. Bordwell, X. Zhang and J. P. Cheng, *J. Org. Chem.*, 1991, **56**, 3216; (b) F. G. Bordwell, *Acc. Chem. Res.*, 1988, **21**, 456; (c) F. G. Bordwell, G. E. Drucker and H. E. Fried, *J. Org. Chem.*, 1981, **46**, 632.
8. L. Wang, X. He, Y. Guo, J. Xu and S. Shao, *Org. Biomol. Chem.*, 2011, **9**, 752.
9. J. Kang, M. Choi, J. Y. Kwon, E. Yeol and J. Yoon, *J. Org. Chem.*, 2002, **67**, 4384.
10. R. Martinez, A. Espinosa, A. Tarraga and P. Molina, *Tetrahedron*, 2008, **64**, 2184.
11. P. Kaur, S. Kaura and K. Singh, *Org. Biomol. Chem.*, 2012, **10**, 1497.
12. (a) B. P. Bandgar, A. V. Patil and V. T. Kamble, *Arkivoc*, 2007, **xvi**, 252.; (b) M. Hosseini-Sarvari, *Synth. Commun*., 2008, **38**, 832; (c) V. T. Kamble, K. R. Kadam, N. S. Joshi and D. B. Muley, *Catal. Commun.,* 2007, ***8,*** 498; (d) K. P. Boroujeni and K. Parvanak, *Chinese Chem. Lett.* 2011, **22**, 939; (e) S. R. Mendes, S. Thurow, M. P. Fortes, F. Penteado,; E. J. Lenardão, D. Alves, G. Perin and R. G. Jacob, *Tetrahedron Lett.,* 2012, **53**, 5402; (f) D. M. Pore, U. V. Desai T. S. Thopate and P. P. Wadgaonkar, *Arkivoc,* 2006, **xii**, 75; (g) M. Chakrabarty, N. Ghosh, R. Basak and Y. Harigaya, *Tetrahedron Lett*., 2002, **43**, 4075; (h) K. Ghodrati1, S. H. Hosseini, R. Mosaedi, C. Karami, F. Maleki, A. Farrokhi and Z. Hamidi, *Int. Nano Lett.,* 2013, **3**, 1; (i) C. Karami, H. Ahmadian, M. Nouri, F. Jamshidi, H. Mohammadi, K. Ghodrati, A. Farrokhi and Z. Hamidi, *Catal. Commun.* 2012, **27,** 92; (j) M. M. Heravi, K.

Bakhtiari and Azadeh Fatehi, *Iran. J. Org. Chem.,* 2009, **2**, 80; (k) F. Shirini, M. Abedini, M. Mamaghani and A. Rahmani nia, *Iran. J. Cat.,* 2012, **2**, 191; (l) D. K. Sharma, A. Hussain, M. R. Lambu, S. K. Yousuf, S. Maiety, B. Singh and D. Mukherjee, *RSC Adv.*, 2013, **3**, 2211.

13. I. V. Kozhevnikov, *Chem. Rev.,* 1998, ***98,*** 171.
14. (a) R.S. Drago, J.A. Dias and T.O. Maier, *J. Am. Chem. Soc.*, 1997, **119,** 7702; (b) J.A. Dias, S.C.L. Dias and N.E. Kob, *J. Chem. Soc. Dalton Trans*., 2001, **3**, 228.
15. Y. Habibi, L. A. Lucia and O. *J.* Rojas, *Chem Rev*., 2010, **110**, 3479.
16. (a) J.S. Yadav, B.V. S. Reddy and A. S. Reddy, *J. Mol. Cat. A: Chem.*, 2008, **280,** 219; (b) M. Kaur, S. Sharma and P. M. S. Bedi, *Chinese J. Cat.*, 2015,**36**, 520; (c) G. D. K. Kumar and S. Baskaran, *J.Org. Chem. ,*2005, **70**, 4520; (d) G. D. K. Kumar and S. Baskaran, *Syn. Lett.*, 2004, **10**, 1719.
17. N. Mizuno and M. Misono, *Chem. Rev.,* 1998**,** ***98,*** 199.
18. (a) N. Mizuno and M. Misono, *J. Phys. Chem.*, 1989, **93**, 3334; (b) N. Mizuno, T. Watanabe and M. Misono, *J. Phys. Chem.*, 1990, **94**, 890.
19. B. B. Bardin and R. J. Davis, *Appl. Catal A: General,* 2000, **200**, 219.
20. (a) Y. Hirano, K. Inumaru, T. Okuhara and M. Misono, *Chem Lett.*, 1996, **25**,1111; (b) K. Y. Lee, T. Arai, S. Nakata, S. Asaoka, T. Okuhara and M. Misono, *J. Am. Chem. Soc.*, 1992, 2836.
21. A. Ganguly, B. K. Paul, S. Ghosh, S. Kar and N. Guchhait, *Analyst,* 2013, **138**, 6532.
22. A. Ganguly, S. Jana, S. Ghosh, S. Dalapati and N. Guchhait, *Spectrochim. Acta Part A***,** 2013, **112**, 237.
23. B. K. Paul and N. Guchhait, *J. Phys. Chem. B*, 2011, **115**, 11938.
24. (a) T. D. Gauthier, E. C. Sham, W. F. Guerln, W. R. Seltz and C. L. Grant, *Environ. Sci. Technol.*, 1986, **20**, 1162; (b) C. A. Parker, Photoluminescence of Solutions; Elsevier: New

York, 1968, pp 220-232; (c) J. R. Lakowicz, Principles of Fluorescence Spectroscopy; Plenum: New York, 1983.

25. (a) S. Dalapati, S. Jana, M. A. Alam, N. Guchhait, *Sens. Actuators B: Chem.*, 2011, **160**, 1106; (b) S. Dalapati, S. Jana, N. Guchhait, *Chem. Lett.,* 2011, **40**, 279.